

Structural and optical characteristics of tantalum oxide grown by pulsed Nd:YAG laser oxidation

E. Atanassova, G. Aygun, R. Turan, and Tz. Babeva

Citation: *Journal of Vacuum Science & Technology A* **24**, 206 (2006); doi: 10.1116/1.2165656

View online: <http://dx.doi.org/10.1116/1.2165656>

View Table of Contents: <http://scitation.aip.org/content/avs/journal/jvsta/24/2?ver=pdfcov>

Published by the AVS: Science & Technology of Materials, Interfaces, and Processing

Articles you may be interested in

[Infrared optical properties of amorphous and nanocrystalline Ta₂O₅ thin films](#)

J. Appl. Phys. **114**, 083515 (2013); 10.1063/1.4819325

[Embedded argon as a tool for sampling local structure in thin plasma deposited aluminum oxide films](#)

J. Appl. Phys. **112**, 103306 (2012); 10.1063/1.4767383

[Optical characteristics of pulsed laser deposited Ba_{0.8}Sr_{0.2}TiO₃ thin films grown on fused quartz substrate](#)


AIP Conf. Proc. **1451**, 139 (2012); 10.1063/1.4732393

[Preparation of \$\alpha\$ -Al₂O₃ thin films by electron cyclotron resonance plasma-assisted pulsed laser deposition and heat annealing](#)

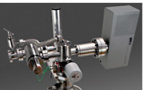
J. Vac. Sci. Technol. A **26**, 380 (2008); 10.1116/1.2899569

[Optical and structural properties of siliconlike films prepared by plasma-enhanced chemical-vapor deposition](#)

J. Appl. Phys. **97**, 023533 (2005); 10.1063/1.1830092



Instruments for Advanced Science

 <p>Gas Analysis</p> <ul style="list-style-type: none">dynamic measurement of reaction gas streamscatalysis and thermal analysismolecular beam studiesdissolved species probesfermentation, environmental and ecological studies	 <p>Surface Science</p> <ul style="list-style-type: none">UHV TPDSIMSend point detection in ion beam etchelemental imaging - surface mapping	 <p>Plasma Diagnostics</p> <ul style="list-style-type: none">plasma source characterizationetch and deposition process reactionkinetic studiesanalysis of neutral and radical species	 <p>Vacuum Analysis</p> <ul style="list-style-type: none">partial pressure measurement and control of process gasesreactive sputter process controlvacuum diagnosticsvacuum coating process monitoring
--	---	---	---

Contact Hiden Analytical for further details:
W www.HidenAnalytical.com
E info@hiden.co.uk
CLICK TO VIEW our product catalogue

Structural and optical characteristics of tantalum oxide grown by pulsed Nd:YAG laser oxidation

E. Atanassova

Institute of Solid State Physics, Bulgarian Academy of Sciences, Sofia 1784, Bulgaria

G. Aygun^{a)}

*Department of Physics, Middle East Technical University, TR-06531 Ankara, Turkey
and Department of Physics, Izmir Institute of Technology, TR-35430 Urla, Izmir, Turkey*

R. Turan

Department of Physics, Middle East Technical University, TR-06531 Ankara, Turkey

Tz. Babeva

Central Laboratory of Photoprocesses, Bulgarian Academy of Sciences, Sofia 1113, Bulgaria

(Received 2 June 2005; accepted 12 December 2005; published 8 February 2006)

Tantalum pentoxide (Ta_2O_5) thin films (20–50 nm) have been grown by 1064 nm Nd:YAG laser oxidation of Ta film deposited on Si. The chemical bonding, structure, and optical properties of the films have been studied by Fourier transform infrared spectroscopy, x-ray diffraction, and reflectance measurements at normal light incidence in the spectral range of 350–800 nm. The effect of the substrate temperature (250–400 °C) during oxidation and its optimization with respect to the used laser beam energy density (3.2–3.4 J/cm² per pulse) is discussed. It is established that the substrate temperature is a critical factor for the effectiveness of the oxidation process and can be used to control the composition and amorphous status of the films. The film density explored by refractive index is improved with increasing film thickness. The refractive index of the layers grown under the higher laser beam energy density and at substrate temperature of 350–400 °C was found to be close to the value of bulk Ta_2O_5 . The films are amorphous at substrate temperature below 350 °C and possessed an orthorhombic (β - Ta_2O_5) crystal structure at higher temperatures. The thinner layers crystallize at a little higher temperature. © 2006 American Vacuum Society.

[DOI: 10.1116/1.2165656]

I. INTRODUCTION

In order to overcome the scaling limit of conventional SiO_2 -based insulators due to high tunneling currents and reliability concerns, high permittivity (high- κ) materials, such as single metal oxides and their silicates as well as ferroelectrics, are being developed as alternative dielectrics in high-density metal-oxide-semiconductor field-effect transistors (MOSFETs) and dynamic random access memories (DRAMs).¹ In that respect, Ta_2O_5 is considered as the promising candidate to replace SiO_2 as a dielectric in storage capacitors of Gigascale DRAMs, (sub-100 nm technology node).^{1,2} It has gained the attention as a memory dielectric mainly due to its maturity in storage capacitors, namely, the excellent step coverage characteristics and high dielectric constant combined with relatively low leakage currents enabling high values of storage charge. After many years of development, the Ta_2O_5 -based DRAMs are being produced by some manufacturers.² In consequence, a number of compatible methods such as rf sputtering, thermal oxidation of Ta film, a variety of chemical-vapor deposition techniques, ion-beam deposition, atomic layer deposition, pulsed laser deposition have been developed to fabricate Ta_2O_5 films.^{2–19} Investigations on the production methodology continue in

competition with alternative solution and each method exhibits advantages and disadvantages in terms of, mainly, electrical properties that are essential for DRAM applications. It is not yet clear which method will be chosen as the best one with respect to the storage capacitor applications because each fabricated method strongly affects the structural and electrical properties of the Ta_2O_5 . The prospect of replacing SiO_2 as a dielectric in DRAMs is a challenge considering that SiO_2 is an excellent dielectric material from the manufacturing point of view. Among the various fabrication methods, the technique of pulsed laser oxidation (PLO) is of a special interest, in general for high- κ dielectrics, mainly by two reasons: (i) it has potential for nanoscale application as a technique of local oxidation of small spots and (ii) since PLO operates at low substrate temperatures, it can minimize a number of problems which occur at high processing temperatures of most high- κ dielectrics (and, in particular, of Ta_2O_5) such as undesirable reactions of the dielectrics with underlying Si resulting in a reduction of the benefits of high- κ material. If PLO meets the requirements for producing high-quality films with high dielectric constant, this would have considerable impact on the future high- κ dielectric technology. It is, then, worthwhile to investigate the optimization of the parameters of PLO to obtain the best methodology for the future applications. At present, there is a limited amount of experimental data for the properties of laser-

^{a)}Author to whom correspondence should be addressed; electronic mail: aygun@newton.physics.metu.edu.tr

grown Ta₂O₅ from the storage capacitor DRAM application point of view. This article presents results for structural and optical properties of Ta₂O₅ formed by pulsed Nd:YAG (yttrium-aluminum-garnet) laser oxidation of Ta film on Si. Special attention is paid to the influence of the substrate temperature on the effectiveness of the oxidation process in terms of structural perfections, amorphous status of the films, and their refractive index values. The properties of laser-grown thin Ta₂O₅ films (20–50 nm) were characterized using Fourier transform infrared (FTIR) spectroscopy and reflectance measurements at normal light incidence. The presence of crystal phase(s) in the layers was determined by x-ray diffraction (XRD) method.

II. EXPERIMENTAL PROCEDURE

The p-type (100) 15–17 Ω cm Si wafers were used as substrates. After conventional chemical cleaning of the wafers, tantalum films with a thickness from 10 to about 20 nm were deposited on Si by rf sputtering of tantalum target (99.99% purity) in an Ar atmosphere, (the system's base pressure was 6×10^{-4} Pa, the working gas pressure was 3 Pa, rf power density was 2.2 W/cm², and the deposition rate was 9.3 nm/min; the substrate was not intentionally heated during the tantalum deposition and presumably remained at temperatures close to room temperature). Subsequently, the samples were laser oxidized in vacuum chamber which was evacuated to a base pressure below 0.13 Pa. The substrate was heated to temperatures between 250 and 400 °C during the oxidation. O₂ gas was introduced into the chamber (working gas pressure p was 123 Pa) after reaching the desired substrate temperature, T_s . The Nd:YAG laser with multiple shots corresponding to applied time durations at 1064 nm, (EKSPLA Pulsed Laser NL301) was used to induce the oxidation. The laser output is composed of a pulse train with individual pulses typically of 4.7 ns. More details on the laser system and laser parameters can be found in Refs. 20 and 21, where we reported data of Nd:YAG laser-oxidized thin SiO₂ films showing parameters close to thermally grown SiO₂. The approach used is only briefly described here. A computer-controlled X-Y scanner system was used to direct the laser beam on a certain region on the substrate with controllable dimensions. By means of the scanner system, the laser beam was scanned over an area on the substrate of approximately 4×4 mm² and it can be further reduced or increased by the software. The speed of the scanner system is 0.3 mm/s. The main laser fluence varied in the range between 3.2 and 3.4 J/cm² per pulse. The oxide thickness, d , and the refractive index, n , of the oxide layers obtained were initially determined by single wavelength ellipsometry, ($\lambda = 632.8$ nm); the films with $d = 20$ –50 nm were studied. Additionally, both the refractive index and the film thickness were determined²² with high accuracy in the spectral range $\lambda = 350$ –800 nm, using reflectance measurements (Varian Cary 5E spectrophotometer with an accuracy of 0.5%) at normal light incidence. n and d of the layer were obtained by minimization of the objective function using the substrate trust region method based on the interior-reflective

Newton method.²³ More details on the calculating procedure used can be found elsewhere.^{21,22} The thickness, dispersion energy, and the single-oscillator energy were varied until a good fit between the measured and calculated values of reflectance was found (accuracy better than 0.5%). The fit was accepted as successful when a good enough accordance (as good as 1 nm) between ellipsometrically measured and obtained after this fitting thickness was achieved. The preliminary experiments showed that the laser oxidation of a tantalum film with a thickness of about $d/2$ resulted in the formation of a tantalum-oxide film with a thickness about d . Laser exposure times in the range of about 30–60 min were used. However, we have observed that the properties of the oxide layer do not have a significant change between 30 and 60 min laser exposure times. Therefore, almost all time durations in the figures have 30 min laser oxidation times. A FTIR spectrometer (BRUKER Equinox 55) was used to obtain information on both the chemical composition and the structure of the films as a function of various oxidation parameters. The crystallinity of the films was examined by taking XRD patterns (Rigaku Miniflex system equipped with Cu $K\alpha$ radiation of average wavelength 1.54059 Å). The patterns were analyzed by a computer software and ICDD database which includes the diffraction patterns of well-known structures. The peak matching process was carried out based on the observed peak positions at specific 2θ values and relative intensities of the peaks.

III. RESULTS AND DISCUSSION

A. FTIR spectra

The FTIR spectra produced from laser-oxidized layers with initial 10 nm Ta films on Si are discussed in this section. Samples with 20 nm Ta layer and their oxidation behavior at both different T_s and laser beam energy density, P , are similar to those presented here. The spectra were taken between 400 and 4000 cm⁻¹, but since the low wavenumber region (< 1100 cm⁻¹) is more important for detection of tantalum-oxide-related bonds, only the region of 400–1200 cm⁻¹ is presented in the figures. OH peaks (around 3300–3400 cm⁻¹) for all the samples without clear dependence on T_s and P are detected. This signal is, however, negligible, suggesting that the films are almost moisture poor. It is expected that postoxidation annealing will remove the little amount of moisture.

Figure 1(a) shows the evolution of FTIR spectra of oxide layers for which the laser beam energy density was kept constant at 3.2 J/cm² and T_s was varied between 250 and 400 °C. At the lowest substrate temperature, the effect of laser oxidation is very poor; only a small absorption line around 650 cm⁻¹ associated with Ta–O–Ta and Ta–O stretching modes are seen in the spectrum. As T_s increases to 300 °C, a shoulderlike band appears in 480–560 cm⁻¹ region and the absorption at 650 cm⁻¹ becomes more pronounced. With further increasing of T_s , this line is formed as a dominant absorption feature between ~ 650 and 720 cm⁻¹. These changes in the spectrum indicate the enhancement

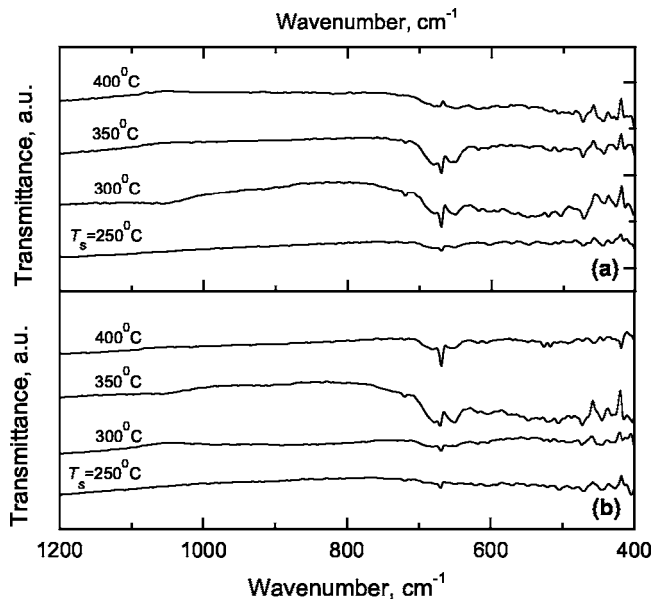


FIG. 1. FTIR spectra of the layers obtained at various substrate temperatures and laser beam energy densities of (a) 3.2 J/cm^2 and (b) 3.3 J/cm^2 .

of the presence of the tantalum oxide(s) in the layers.^{15,24} The character of the shoulder does not apparently change at $T_s > 300^\circ\text{C}$ and the spectra corresponding to T_s of 350 and 400°C are indistinguishable in this region. The feature at 670 cm^{-1} which is superimposed on the main broad signal is associated with vibration modes of CO_2 resulting probably from the air ambient during the measurements. We will not discuss this peak further, since it is not related to the oxidation process itself. On the other hand, the absorption dip is unexpectedly smaller for the highest substrate temperature sample than those of the samples oxidized at lower T_s . This is believed to result from variations in the laser beam energy density and focusing system. This behavior is not seen in the next sample set presented below. The effect of T_s upon the spectra of the films obtained at laser beam energy density of 3.3 J/cm^2 is shown in Fig. 1(b). The tendency of variation of the spectra is similar to that in Fig. 1(a), namely, the sample oxidized at the lowest substrate temperature exhibits only negligible absorption at around 650 cm^{-1} ; the intensity of this line increases a little and a wide shoulderlike absorption band appears between 450 and 550 cm^{-1} , when $T_s = 300^\circ\text{C}$. At $T_s = 350$ and 400°C , this broad absorption band reduces whereas, the intensity of the peak at 650 cm^{-1} increases. These results suggest that the layers become denser with increasing T_s and the effect is obviously stronger for a higher laser beam energy density. It emerges that the substrate temperature during laser oxidation is the critical factor determining the effectiveness of the process, and the effective laser oxidation of Ta at $T_s = 250^\circ\text{C}$ is not possible. The impact of substrate temperature on the oxidation process implies that the oxygen diffusion can be invoked to explain the mechanism of oxidation. The laser oxidation process, however, goes under very complex conditions and it is not possible to make an explicit inference on the mechanism of oxidation based only on the present experimental data. More complex

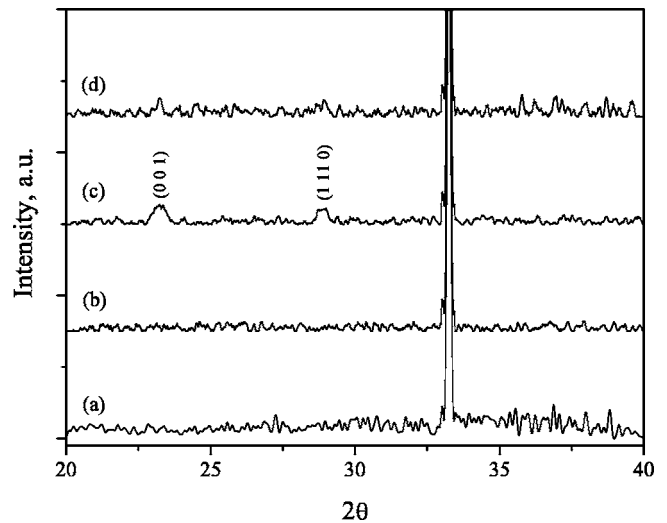


FIG. 2. XRD spectra of Ta_2O_5 layers (22 and 41 nm) grown at various T_s : $d=22 \text{ nm}$, $T_s=300^\circ\text{C}$ (a); 350°C (b); 400°C (c); $d=41 \text{ nm}$, $T_s=350^\circ\text{C}$, 400°C (d); ($P=3.3 \text{ J/cm}^2$).

analysis (including the effect of partial pressure of oxygen) is necessary to clarify the mechanism of oxidation and to determine the dominant oxidizing component of the process and such an analysis is beyond the scope of this work.

Under the light of experimental evidences presented, we can conclude that the laser oxidation of Ta film on Si takes place without presence of significant amount of suboxides. Only for $T_s=300, 350^\circ\text{C}$, $P=3.3 \text{ J/cm}^2$, [Fig. 1(b)] the shoulder, respectively, within $770\text{--}1050 \text{ cm}^{-1}$ and $850\text{--}1000 \text{ cm}^{-1}$, is assigned to the presence of suboxides^{15,24} in the films obtained at these conditions. A weak band also emerges at $\sim 900 \text{ cm}^{-1}$ in the spectra of the films oxidized at 250°C .

As is known,^{1,2,6-8} the formation of ultrathin SiO_2 -based layer at the interface with Si is unavoidable during formation of a number of high- κ dielectrics on Si, (Ta_2O_5 is not an exception). We have no strong indication for the presence of Si-O stretching band in the spectra (typically around $1070\text{--}1100 \text{ cm}^{-1}$). Only the film obtained at 350°C , [Fig. 1(b)] exhibits very small bands in this region which can be attributed to the presence of Si-O-Si stretching vibration mode.²⁵ These peaks do not change with varying P and have negligible intensity which means that if there is an interfacial layer containing SiO_2 and/or intermediate oxidation states of Si, it is extremely thin.

B. XRD results

Figure 2 presents the XRD spectra of laser-oxidized Ta films grown at various substrate temperatures for two representative tantalum oxide thicknesses (~ 20 and 40 nm). All of the samples corresponding to certain T_s and d showed identical spectra. No diffraction peaks except for those from Si substrate (the intensive peak at 33.26°) were observed in the spectra of thinner films (22 nm) obtained at $T_s=300$ and 350°C —the shape of the spectra indicates an amorphous structure of Ta_2O_5 . The oxidation, however, at 400°C ,

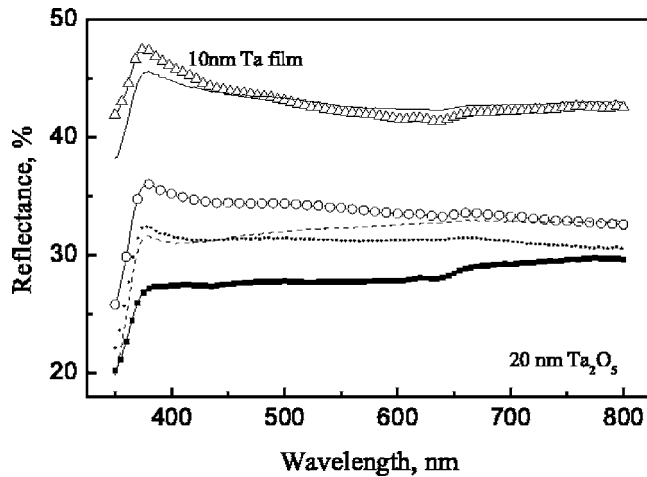


FIG. 3. Reflectance spectra of 20 nm laser-oxidized Ta_2O_5 at various substrate temperatures, $P=3.3 \text{ J/cm}^2$: (—) $T_s=250 \text{ }^\circ\text{C}$, (○-○-○) $T_s=300 \text{ }^\circ\text{C}$, (···) $T_s=350 \text{ }^\circ\text{C}$; (■-■-■) $T_s=400 \text{ }^\circ\text{C}$; $P=3.2, 3.3 \text{ J/cm}^2$; ---- $P=3.2 \text{ J/cm}^2$, $T_s=350 \text{ }^\circ\text{C}$; ($\Delta\Delta\Delta$) reflectance spectrum of 10 nm Ta film on heated substrate, $T_s=250\text{--}400 \text{ }^\circ\text{C}$, (see the text).

induced the crystallization giving rise to specific diffraction lines typical of orthorhombic β phase²⁶ (x-ray diffraction file, Card No. 71-0639). The peaks (at 23.24° and at 28.26°) with small intensity and relatively broad full width at half maximum (FWHM) of 0.635° and 0.471° , respectively, indicate a low level of crystallization.

The spectra of thicker oxide layers ($\sim 40 \text{ nm}$) show no indication of crystallization when T_s is below $350 \text{ }^\circ\text{C}$ —only strong diffraction signal from the substrate is present. The spectrum of the layers oxidized at $350 \text{ }^\circ\text{C}$ (or $400 \text{ }^\circ\text{C}$), Fig. 2(d), shows very small diffraction lines whose positions correspond to reflexes of orthorhombic β phase. Concerning the crystal phase and the shape of XRD spectra, both substrate temperatures are identical. The substrate temperature leading to crystallization is therefore between 350 and $400 \text{ }^\circ\text{C}$ for thinner films (up to $20\text{--}25 \text{ nm}$) and close to $350 \text{ }^\circ\text{C}$ for thicker films ($\sim 40 \text{ nm}$). The polycrystalline Ta_2O_5 can be identified as the low temperature $\beta\text{-Ta}_2\text{O}_5$ phase, whereas, the peaks in the spectra of thicker films are not well pronounced which reflect the very weak extent of crystallization. Then, it can be concluded that at $T_s < 350 \text{ }^\circ\text{C}$, Ta_2O_5 obtained by laser oxidation is amorphous being independent of the film thickness (up to $\sim 40 \text{ nm}$). At higher temperatures, the films crystallize—the thicker layers crystallize at lower T_s as compared to the thinner one. Obviously, the higher substrate temperature stimulates the formation of crystal phase, but the effect is definitely weak and even weaker for greater oxide thicknesses.

In terms of XRD analysis, no evidence was found for tantalum silicide formation or segregation of metallic constituents, which could act as a leakage current enhancement factor.

C. Reflectance spectra and refractive index

Figure 3 shows the influence of the substrate temperature on the reflectance spectra of 20 nm Ta_2O_5 films oxidized at

laser beam energy density of 3.3 J/cm^2 . The small changes in P have no effect on the reflectance of the layers obtained at $T_s=350$ and $400 \text{ }^\circ\text{C}$; the curves corresponding to $P=3.2$ and 3.3 J/cm^2 are almost the same. Reflectance spectrum for 10 nm Ta film on Si, (i.e., a spectrum of the initial sample before laser oxidation) is also presented. As T_s increases from 250 to $400 \text{ }^\circ\text{C}$, the reflectance R decreases and the effect is more pronounced at smaller wavelengths, λ : the decrease ΔR in R is $17\%\text{--}18\%$ in the ultraviolet region ($\lambda=350\text{--}400 \text{ nm}$), and $\Delta R=13\%\text{--}17\%$ in the visible one. The reflectance drop indicates an increase in the optical thickness, which is defined as the product of the refractive index, n , of the layer and its physical thickness, d . The reflectance, R , decreases with increasing T_s and the curves are practically shifted parallel to each other with ΔR of $\sim 10\%$. The highest drop of R , in the whole spectral range, is detected when T_s changes from 250 to $300 \text{ }^\circ\text{C}$, implying that the active oxidation starts somewhere at the substrate temperature between 250 and $300 \text{ }^\circ\text{C}$. Additional evidence for this suggestion is seen from the reflectance spectrum of a Ta film on Si after heating the substrate without laser oxidation, (Fig. 3). The spectrum of metallic Ta does not change with varying T_s from 250 to $400 \text{ }^\circ\text{C}$ indicating that there is no any thermal oxidation without laser action. The spectrum of Ta film and the laser-oxidized layer at $250 \text{ }^\circ\text{C}$ are also the same, i.e., even though there are small optical thickness variations, the reflectance is not sensitive to them. The laser-oxidized films exhibit, however, considerably different behavior than metallic Ta, when the oxidation takes place at T_s higher than $250 \text{ }^\circ\text{C}$. So, we can conclude that the active oxidation process starts, i.e., the transition from metallic Ta to tantalum oxide, at T_s greater than $250 \text{ }^\circ\text{C}$. Furthermore ($T_s \geq 300 \text{ }^\circ\text{C}$), an increase of T_s with a step of $50 \text{ }^\circ\text{C}$ resulted in a constant but smaller reduction of R , ($\Delta R \sim 4\%$ as compared to ΔR when T_s changes from 250 to $300 \text{ }^\circ\text{C}$). In fact, the reflectance behavior is related with changes of optical thickness, nd , of the layer. Since R is a periodical function of nd with a periodicity of $\lambda/2$, it changes with variation of nd from zero to $\lambda/4$, and depends on the ratio between refractive index n of the layer and of the substrate, n_{sub} , respectively, (R decreases when $n/n_{\text{sub}} < 1$ and vice versa). If we suppose that the values of n are close to $2\text{--}2.2$, which are the typical values of stoichiometric Ta_2O_5 ,^{7,16,25} the optical thickness will vary from $\lambda/8$ to $\lambda/18$ in the whole spectral range and it will be generally smaller than $\lambda/4$. Considering that $n/n_{\text{sub}} < 1$, ($n_{\text{sub}}=5.60\text{--}3.66$ in the used spectral range for Si wafer), the decay of R could be attributed to the increase of optical thickness. As far as the films' thickness is constant (20 nm) independently of T_s an increase of n is the only possible explanation of the greater values of nd at higher T_s . It should be noted, however, that it is hard to draw a conclusion considering only the R spectral behavior because of the sophisticated relationship between R and n . The key role of the refractive index in these characteristics of the optical thickness is fairly plausible. The values of n , obtained after experimental reflectance spectra fitting, with respect to λ between 400 and 800 nm for three substrate

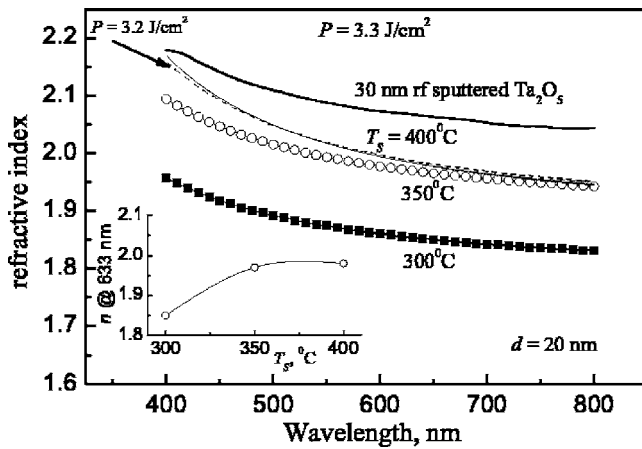


FIG. 4. Refractive index as a function of λ for laser-oxidized films obtained at different conditions; $n(\lambda)$ dependence of rf-sputtered Ta_2O_5 (taken from Ref. 27) is shown for comparison. The inset shows variation of n at 633 nm with T_s .

temperatures are presented in Fig. 4. The data for two values of P , ($T_s=400^\circ\text{C}$) are also shown as well as a curve of rf-sputtered Ta_2O_5 (30 nm),²⁷ for comparison. All spectra with exception of the case $T_s=250^\circ\text{C}$ are fitted very well using the model of single oxide layer. This confirms the assumption that the active laser oxidation obviously occurs at $T_s>250^\circ\text{C}$. The ellipsometrical values of n are 1.9–2 for the 10 nm Ta oxidized films and 1.95–2.1 for 20 nm ones and these are in a very good accordance with the calculated values at $\lambda\approx 633$ nm. Generally, the dispersion curves exhibit a typical wavelength dependence of n for non- or slightly absorbing film, i.e., n decreases with increasing λ and tend to saturate at higher λ ($\lambda\geq 600$ nm). n increases with T_s and the effect is more pronounced when T_s varies from 300 to 350 $^\circ\text{C}$, i.e., the film undergoes a structural transformation upon oxidizing at T_s between 300 and 350 $^\circ\text{C}$, while the refractive index is improved slightly for the highest T_s . The degree of the improvement depends on λ : the effect is stronger for the shorter wavelength region, (~ 400 –600 nm); the maximum increase of n , from 2.09 to 2.17 is detected at $\lambda=400$ nm. The impact of T_s on refractive index suggests that the growth processes have different controlling mechanisms at various substrate temperatures resulting in the layers with varying density, (i.e., different n). The dependence of n on T_s at a photon energy of 1.96 eV, ($\lambda=633$ nm), presented as the inset of Fig. 4, confirms that the influence of T_s is essential in the range 300–350 $^\circ\text{C}$, where n arises with 0.12, achieving the value of 1.98, similar to values reported for as-fabricated Ta_2O_5 films obtained by other methods.^{6,7,16,27} Further, the highest T_s does not lead to any increase of refractive index at 633 nm. Obviously, the dense enough as-grown oxides can be achieved at $T_s=350$ –400 $^\circ\text{C}$. As is seen from Fig. 4, the small variations of laser energy density (at identical T_s) do not influence on refractive index. It is worth noting that the refractive indices of laser-oxidized films, even for the highest T_s , do not reach those corresponding to rf-sputtered films with similar thicknesses, indicating that the laser oxidation provides lower re-

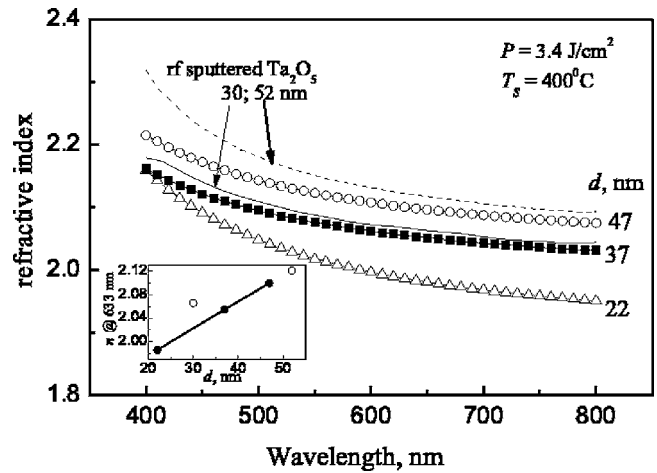


FIG. 5. Dependence of refractive index on λ for the laser-oxidized films with various physical thickness. The curves corresponding to two rf-sputtered Ta_2O_5 samples (taken from Ref. 27) are given for comparison. The inset shows the variation of n vs d ; ● laser oxidized; ○ sputtered Ta_2O_5 .

fractive index as compared to the deposition process by rf sputtering of Ta target in Ar+O₂ mixture.^{6,27} The poor density, high porosity, and oxygen deficiency of the layers are the possible reasons for the lower n values. However, both types of Ta_2O_5 obey stronger dispersion in the shorter wavelength region, ≈ 400 –650 nm. This could be attributed to the presence of suboxides which causes the absorption edge to shift to larger wavelengths or to the large surface roughness. The suggestion of suboxides is a simpler explanation and it is completely consistent with the data of Auger and x-ray photoelectron spectroscopy (XPS) analyses of rf-sputtered samples⁷ where the presence of Ta suboxides was demonstrated through the depth of the layers. On the other hand, FTIR analysis indicates relatively weak presence of suboxides in laser-grown Ta_2O_5 . In order to clarify this point, the detailed XPS measurements, including depth profiles, are now in progress for the laser-oxidized samples.

The index of refraction increases as the film thickness increases. The dispersion curves of n for three oxide thicknesses as measured ellipsometrically, (under otherwise the identical conditions, $P=3.4$ J/cm², $T_s=400^\circ\text{C}$, corresponding to more efficient oxidation process) are presented in Fig. 5. The data of as-deposited rf-sputtered 30 and 52 nm-thick Ta_2O_5 films²⁷ are also given for comparison. The highest refractive index is obtained for the thickest laser-oxidized layer (47 nm): the values of n are very close to those of 52 nm rf-sputtered Ta_2O_5 , for $\lambda\geq 550$ nm (the difference is only 0.01–0.03), despite the laser-oxidized film being a little thinner. The values of n in the whole spectral range for both 37 nm laser-oxidized Ta_2O_5 and 30 nm sputtered one are almost the same. Therefore, the results suggest that the laser oxidation of Ta films to thicknesses of Ta_2O_5 above ~ 35 nm provides layers with the same density, (in terms of refractive index) as rf-sputtered Ta_2O_5 . Consequently, it can be expected that the similar chemical composition of the two types of oxides. The inset of the figure indicates the corresponding changes of refractive index at 633 nm with film thickness for

laser-oxidized and rf-sputtered Ta₂O₅. Generally, the thickness dependence of n seems to be attributed to the better density of thicker films, (densified oxides with a better stoichiometry), resulting in a reduction of interatomic spacing. Since n is proportional to the electronic polarizability which is inversely proportional to the interatomic spacing, the reduction of this spacing for thicker films directly results in an increase of their refractive indices. The observed weaker dispersion of the thicker films as compared to the thinnest one suggests the improved stoichiometry of thick films too.

IV. CONCLUSION

We have successfully demonstrated Nd:YAG laser-assisted growth of Ta₂O₅ films (20–50 nm) by oxidation of deposited Ta film on Si by employing FTIR, XRD, and reflectance spectra analyses. The laser oxidation provides films whose structure, amorphous status, optical thickness, and refractive index can be effectively controlled by the substrate temperature (250–400 °C). The active oxidation starts between 250 and 300 °C of substrate temperature and further the increase of substrate temperature leads to progressive improvement of film's density. The XRD data showed that the films grown at or below 350 °C are amorphous and the films grown at higher temperature are polycrystalline with orthorhombic structure. In fact, the substrate temperature leading to crystallization depends on the thickness of the layers; for the thinner layers (which are of practical interest) it is higher being between 350 and 400 °C. The goal result here, however, is that in all cases the crystallization effect is definitely weak which can be very important for high- κ application of laser-grown Ta₂O₅. Therefore, we can conclude that the most desirable growth condition with respect to amorphous status of the films, their stoichiometry and refractive index (i.e., dense films) is at substrate temperature close to the temperature (but without crossing it) when the crystallization starts. We also have indication that the lower- κ interfacial layer at Si is extremely thin which means that this oxidation technique has the potential as an enabling technology for nanoscale high- κ dielectric-based devices. The interfacial perfection will help to reduce the oxide equivalent thickness.

The refractive index increases with increasing the film thickness accompanied by a decrease of the dispersion implying a higher level of film densification and improved stoichiometry for thicker films. The thickest layers used here (45–50 nm) have refraction indices close to the typical values of bulk stoichiometric Ta₂O₅. All quantitative suboxide aspects of the layers, however, require a precise XPS analy-

sis including depth profiling. Work is proceeding on this and we hope to report further on this topic in the near future.

ACKNOWLEDGMENTS

This work has been partly supported by Bulgarian National Science Foundation (Project No. F1508) and by TUBITAK (Scientific and Technical Council of Turkey) under Project No. TBAG/U68.

- ¹*International Technology Roadmap for Semiconductors (ITRS)* (Semiconductor Industry Association, San Jose, 2003); <http://public.itrs.net>
- ²A. I. Kingon, J. P. Maria, and S. K. Streffer, *Nature* (London) **406**, 1032 (2000).
- ³S. Kamiyama, P. Lesaicherre, H. Suzuki, A. Sakai, I. Nishiyama, and A. Iskitani, *J. Electrochem. Soc.* **140**, 1617 (1993).
- ⁴S. R. Jeon, S. W. Han, and J. W. Park, *J. Appl. Phys.* **77**, 5978 (1995).
- ⁵J. V. Chrahn, P. E. Hellberg, and E. Olson, *J. Appl. Phys.* **84**, 1632 (1998).
- ⁶E. Atanassova, *Microelectron. Reliab.* **39**, 1185 (1999).
- ⁷E. Atanassova and T. Dimitrova, in *Handbook of Surfaces and Interfaces of Materials*, edited by H. S. Nalwa (Academic, San Diego, CA, 2001), Vol. 4, p. 439.
- ⁸C. Chaneliere, J. L. Autran, R. A. B. Devine, and B. Balland, *Mater. Sci. Eng., R.* **22**, 269 (1998).
- ⁹K. Kukli, J. Aarik, A. Aidla, O. Kohan, T. Uustare, and V. Sammelselg, *Thin Solid Films* **260**, 135 (1995).
- ¹⁰Z. Mingfei, F. Zhengwen, Y. Haijun, Z. Zhuangjian, and Q. Qizong, *Appl. Surf. Sci.* **108**, 399 (1997).
- ¹¹Y. Nishimura, A. Shinkawa, H. Ujita, M. Tsuji, and M. Nakamura, *Appl. Surf. Sci.* **136**, 22 (1998).
- ¹²J. Y. Zhang and I. W. Boyd, *Appl. Surf. Sci.* **168**, 234 (2000).
- ¹³S. Boughaba, G. I. Sproule, J. P. McCaffrey, M. Islam, and M. J. Graham, *Thin Solid Films* **358**, 104 (2000).
- ¹⁴J. Y. Kim, M. C. Nielsen, E. J. Rymaszewski, and T. M. Lu, *J. Appl. Phys.* **87**, 1448 (2000).
- ¹⁵I. W. Boyd and J. Y. Zhang, *Microelectron. Reliab.* **40**, 649 (2000).
- ¹⁶G. D. Wilk, R. M. Wallace, and J. M. Anthony, *J. Appl. Phys.* **89**, 5243 (2001), and references therein.
- ¹⁷J. Y. Zhang, V. Dusastre, and I. W. Boyd, *Mater. Sci. Semicond. Process.* **4**, 313 (2001).
- ¹⁸E. Atanassova, N. Novkovski, A. Paskaleva, and M. Pesovska-Gjorgjevich, *Solid-State Electron.* **46**, 1887 (2002).
- ¹⁹M. Passacantando, F. Jolly, L. Lozzi, V. Salerni, P. Picozzi, S. Santucci, C. Corsi, and D. Zintu, *J. Non-Cryst. Solids* **322**, 225 (2003).
- ²⁰G. Aygun, E. Atanassova, A. Alicakir, L. Ozyuzer, and R. Turan, *J. Phys. D* **37**, 1569 (2004).
- ²¹G. Aygun, E. Atanassova, R. Turan, and Tz. Babeva, *Mater. Chem. Phys.* **89**, 316 (2005).
- ²²Tz. Babeva, S. Kitova, B. Mednikarov, and I. Konstantinov, *Appl. Opt.* **41**, 3840 (2002).
- ²³T. F. Coleman and Y. Li, *SIAM J. Optim.* **6**, 418 (1996).
- ²⁴J. Y. Zhang, Q. Fang, and I. W. Boyd, *Appl. Surf. Sci.* **138–139**, 320 (1999).
- ²⁵J. J. Yu, J. Y. Zhang, and I. W. Boyd, *Appl. Surf. Sci.* **186**, 57 (2002).
- ²⁶x-ray diffraction file, ICDD.
- ²⁷Tz. Babeva, E. Atanassova, and J. Koprinarova, *Phys. Status Solidi A* **202**, 330 (2005).